34th Annual International Conference of the IEEE EMBS
San Diego, California USA, 28 August - 1 September, 2012

A Transcutaneous Power Transfer Interface Based on a Multicoil Inductive Link

S. A. Mirbozorgi, *Student Member, IEEE*, B. Gosselin, *Member, IEEE,* and M. Sawan, *Fellow, IEEE.*

***Abstract*— This paper presents a transcutaneous power transfer link based on a multicoil structure. Multicoil inductive links using 4-coil or 3-coil topologies have shown significant improvement over conventional 2-coil structures for transferring power transcutaneously across larger distances and with higher efficiency. However, such performance comes at the cost of additional inductors and capacitor in the system, which is not convenient in implantable applications. This paper presents a transcutaneous power transfer interface that takes advantage on a 3-coils inductive topology to achieve wide separation distances and high power transfer efficiency without increasing the size of the implanted device compared to a conventional 2-coil structure. In the proposed link, a middle coil is placed outside the body to act as a repeater between an external transmitting coil and an implanted receiving coil. The proposed structure allows optimizing the link parameters after implantation by changing the characteristics of the repeater coil. Simulation with a multilayer model of the biological tissues and measured results are presented for the proposed link.**

I. Introduction

There are several applications in which an implantable electronic device cannot use batteries as primary source of energy. Instead, power must be delivered wirelessly across the skin through an inductive link formed by mutually coupled coils. Inductive coupling is among the safest method to power up implants because it avoids risks of infection and tethering associated with transcutaneous wires.

Inductive power transfer received a lot of attention over the last decade. Such links can deliver sub-micro to mill-watts of power wirelessly across distances of 10 mm to 200 mm [1]-[6]. In such application, improving power transfer efficiency (PTE) and achieving larger coupling distances, without increasing the losses and absorption in biological tissues, is the aim of several researchers. Indeed, safety imposes a maximum absorption rate that limits magnetic field in the body, which shows the importance of increasing the PTE [7].

Inductive power transfer links have been designed and optimized through modeling and analysis of different inductively coupled topologies. Among the exploited techniques for design and analysis are the Coupled Mode Theory (CMT) and the Reflected Load Theory (RLT) [6], [8], which has recently received attention. Moreover, different coils structure and material like wire wound and printed spiral coil, were compared [9], [6].

This work was supported in part by the Natural Sciences and Engineering Research Council of Canada and by the Regroupement Stratégique en Microélectronique du Québec. S. A. Mirbozorgi and B. Gosselin are with the Dept. of Electrical and Computer Eng., Université Laval, Quebec, QC G1V 0A6, Canada (e-mail: sa.mirbozorgi@gmail.com). M. Sawan is with the Dept. of Electrical and Computer Eng., École Polytechnique de Montréal, Montréal, QC H3C 3A7, Canada.

However, inductive links suffer from low-efficiency in general due to the low magnetic coupling (k) between coils, which limits the maximum transferable power. Conventional transcutaneous wireless power transfer systems feature two coils. Coupling between the two coils and their quality factor (Q) are strongly related with the PTE. Increasing the distance between the coils dramatically decreases coupling, thus the PTE. Moreover, the mutual inductance decreases as a function of d^3, where d is the center-to-center distance between the coils [10]. Having large PTE is desirable because it reduces heat dissipation and limits the presence of AC magnetic field in the tissue [7]. Besides, the surrounding biological environment and the presence of parasitic components are known to largely influence the resulting efficiency by changing the link parameters.

Although 2-coil links are an optimal choice for achieving high power delivery at small coupling distances [6], [9], multicoil topologies have recently been proposed to improve power transfer efficiency at longer coupling distance [1], [3], [6]. In addition to allow higher PTE across longer distances, multicoil structures provide more degrees of freedom for optimization of the power link. In the 4-coil structure, a pair of coils is used on the transmitter (TX) side while another pair of coils is used on the receiver (RX) side. A 4-coil system allowed transferring power to an implanted unit over a distance of 10 to 20 cm [1], [6]. The 4-coil technique can compensate for the effects of low-k and low-Q which facilitates the optimization of the power transfer efficiency in the link. Moreover, the PTE of a 4-coil link decreases less with distance compared to conventional 2-coil power transfer systems, and it provides better immunity to variations in the operating frequency [3], [6].

However, although the 4-coil approach increases PTE across large separation distances, it causes a significant reduction in the power delivered to the load (PDL) [6]. Moreover, 4-coil systems require a high driving voltage which can lead to reduced driver efficiency and safety issues [3], [6]. To compensate for these effects, an inductive power transfer link based on a 3-coil topology is proposed in [6]. Such topology provides high PTE as well as higher PDL than the 2- and 4-coil inductive approaches, at large d. In the 3-coil structure, the mutual inductance between the pair of implanted coils plays the role of an impedance matching circuit that can convert any arbitrary load into a value that can maximize the PTE. However, one disadvantage of the 3- and 4-coil inductive links is the increased size of the system, particularly, in the implanted part.

In this paper, the 3-coil structure is utilized to transfer power from a remote coil to an implanted system without increasing the number of component in the implant. The middle coil, which is used as a repeater, plays the role of a

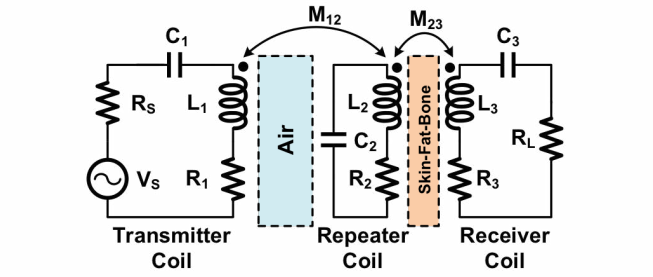

Figure 1. Schematic diagram of the 3-coil inductive link and the place of tissue.

load matching element that conveys the received power from a remote transmitting coil to an implanted receiving coil, through bone, fat and skin. Hence, it takes advantage on the 3-coil method for increasing the separation distance between the transmitter and the receiver coil without increasing the size of the implanted unit compared to a 2-coil inductive link. Thus, the presented structure aims at 1) eliminating supply wire at the transmitter coil location, which is located outside the body, near the implanted area, and 2) giving more degrees of freedom for optimizing the power transfer link. Moreover, in the case of animal research, the proposed topology aims at enabling experimentations with freely moving subjects.

In the following section, we describe the proposed power transfer interface and we present its simulated performance into ADS and HFSS. Then, we present the measurement results in Section III, and we conclude in the last section.

II. Proposed 3-coil based structure

In general, the performance of the 3-coil topology is superior to the 2-coil approach when it is required to simultaneously optimize PTE and PDL over wide separation distances [6], at the cost of additional components. Fig. 1 shows the schematic diagram of the proposed 3-coil transcutaneous inductive link. The coil L_2 and its capacitor are located outside of the body to decrease the size of the implanted unit and give the necessary degrees of freedom to optimize the link after implantation.

First, the feasibility of such topology was investigated using simulation. The PTE and the PDL has been simulated using ADS for different conditions. Fig. 2 and Fig. 3 show the PDL and PTE as a function of k_{12} and k_{23}, respectively (the variation range of k_{12} and k_{23} are chosen considering practical limitations). As shown in Fig. 2, the PDL is increased by increasing the separation distance (d), (decreasing the k_{12}) and sharply decreased for the $k_{12}<0.02$. Also, Fig. 2 shows that when increasing d, the maximum PDL is reached for the lowest k_{23}. Thus, achieving a high PDL while increasing d (decreasing the k_{12}) requires that k_{23} be decreased. Optimizing the inductive link consists in achieving the best PDL and PTE simultaneously. Hence, considering Fig. 2 and Fig. 3, the best case to get the highest PDL and PTE as possible happens between $k_{12}<0.05$ and $0.1<k_{23}<0.3$. Since L_2 is located outside the body, there is no limitation on its size. Moreover, biological tissues (bone, fat and skin), the thicknesses of which vary between individuals, set the minimum separation between L_2 and L_3.

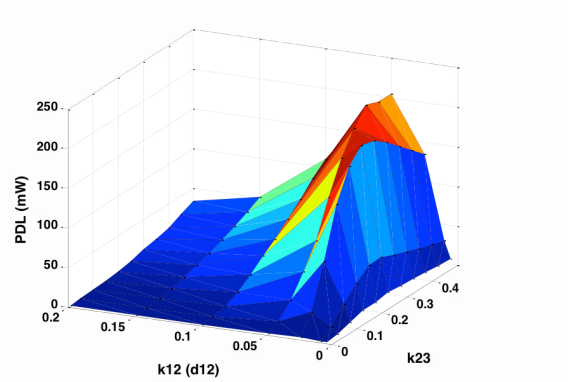

Figure 2. Power delivered to the load (PDL) as a function of k_{12} and k_{23}.

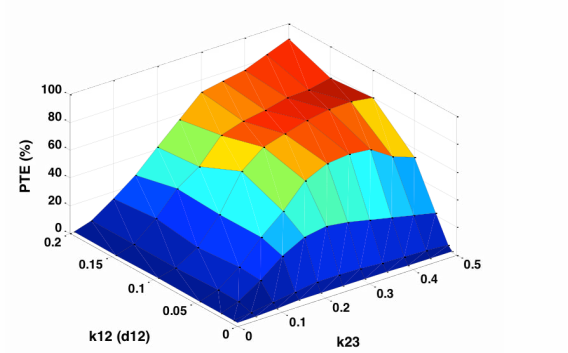

Figure 3. Power transfer efficiency (PTE) as a function of k_{12} and k_{23}.

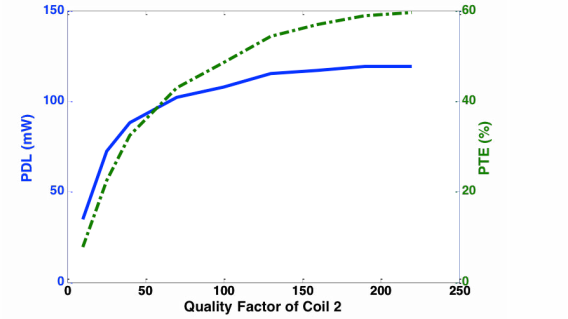

Figure 4. PDL and PTE as a function of quality factor of repeater.

Thus, L_2 can easily be tuned to adjust the link toward arbitrary values of k_{23}. All simulations use a nominal load of 100 Ω, V_S=1V and f_0=13.56 MHz.

Although increasing the inductance L_2 while keeping the quality factor (Q) and k_{23} constant does not increase the PDL and PTE, changing Q has a significant effect on the PDL and PTE, as shown in the Fig 4. To show the ability of the proposed inductive link to increase the transmitted power to the load, the PDL and PTE are presented as a function of V_S (Fig. 5). Fig. 5 shows that although the PDL increases after increasing V_S, the PTE will remain almost constant, which allows transferring higher amount of power to the implanted side. HFSS has been used to extract the parameters of the coils and to simulate the characteristics of the inductive link. A model, which has previously been developed to design a wireless data link in a brain monitoring implant was used to account for the effect of biological tissues between the

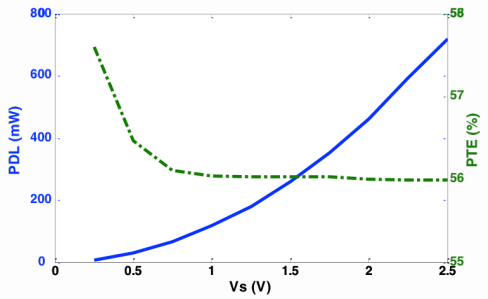

Figure 5. PDL and PTE as a function of V_S.

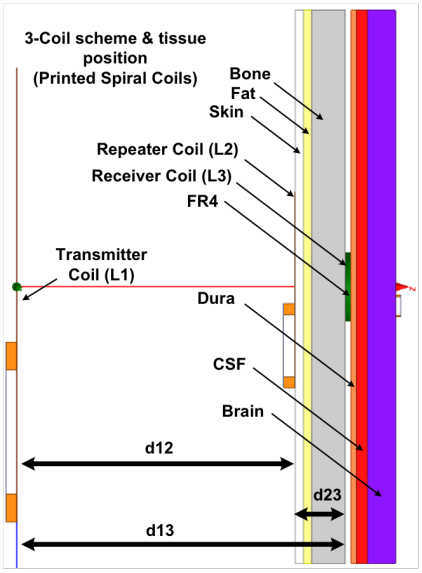

Figure 6. Proposed structure simulated by HFSS.

repeater coil and the receiver coil [11]. Indeed, inductive power transfer is essential in such application since small brain monitoring implants cannot use batteries [12]. The adopted model includes several layers having different dielectric constants and characteristics, which are obtained from [13], [14]. Fig. 6 shows a representation of the coils simulated in HFSS and their locations. Three printed spiral coils are used for L_1, L_2 and L_3, with thickness of 0.035 mm. The specifications of the coils are presented in Table I. To simulate the 3-coil resonance-based inductive link into HFSS and ADS, the repeater coil (L_2) and a parallel capacitor are tuned at the resonant frequency of 13.56 MHz. The same strategy has been employed to operate the implemented link into a test setup to gather experimental measurements. As a result, a significant increase appeared in the coupling between coils (transmitter and receiver coils in the 3-coil topology), and so in the PDL. Simulation results obtained with HFSS are presented in Section III and are compared with measurement results.

III. Measurement Results

The effect of adding a repeater coil between the transmitter and receiver coils (the 3-coil inductive link) on the coil coupling, thus on PDL and PTE, was tested and compared with a conventional 2-coil inductive link.

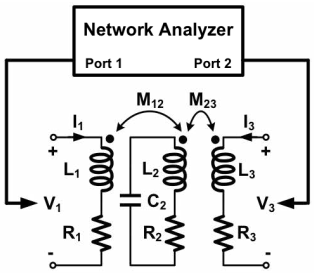

Figure 7: Measurement scheme for inductive link using Network Analyzer while L_2 is tuned at the frequency of 13.56MHz.

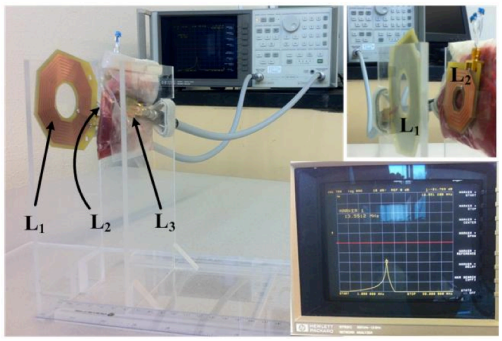

Figure 8. 3-coil inductive link experimental setup used to measure insertion loss (coil coupling).

Table I. Parameters of fabricated printed spiral coils (extracted from HFSS).

Parameters	Symbols	L_1	L_2	L_3
Inductance (µH)	L	3.8	0.88	0.45
Outer diameter (mm)	D_O	70	40	10.5
Number of turns	n	8	5	8
Line width (µm)	w	2000	2000	250
Line spacing (µm)	s	500	500	210
Quality factor	Q	58	63	42

Fig.7 shows the experimental setup exploited to characterize the 3-coil inductive link using a network analyzer. With the proposed approach, only the repeater coil needs to be tuned at the resonant frequency of 13.56 MHz. The network analyzer is used to measure the S-parameter (S12) of the link. The couplings between the coils of the 3-coil inductive link are measured using the experimental setup illustrated in Fig. 8. Printed spiral coils were fabricated on a FR4 substrate using a printed circuit board fabrication process, featuring a thickness of 1.5 mm. The design of the coils was based on the parameters extracted from HFSS. The parameters of the fabricated coils are summarized in Table I.

The S-parameter (S12) (between the transmitter and the receiver coil) gives the insertion loss and the coil coupling (between L_1 and L_2 for the 2-coil and, L_1 and L_3 for the 3-coil structures), from which values is derived the PDL. The network analyzer swept the frequency band ranging from 1 MHz to 30 MHz. The measurement results and the simulation results obtained with HFSS for both the 2- and 3-coils (Fig. 7) link configurations are presented in Fig. 9. As shown in this figure, it is obvious that the coupling factor is drastically increased at the resonant frequency of 13.56 MHz for the 3-coil structure, for a center-to-center distance of 5

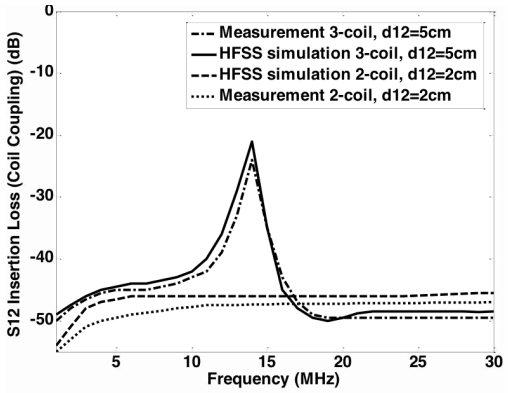

Figure 9. Comparison between measured and simulated (HFSS) values of the coil coupling as a function of frequency for both 2- and 3-coil inductive links.

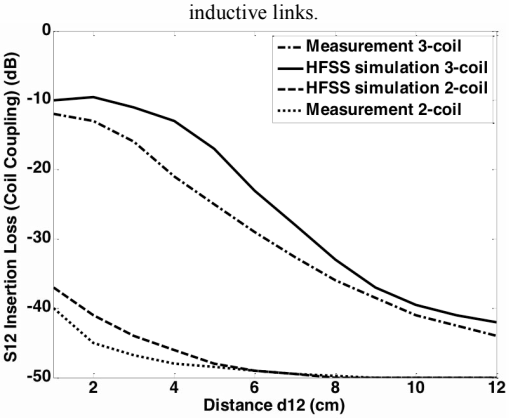

Figure 10. Comparison between measured and simulated (HFSS) values of the coil coupling as a function of distance for both 2- and 3-coil inductive links.

cm between L_1 and L_2 (d_{12}), compared with the 2-coil topology. Similar measurements and simulation results are obtained for the 2-coil topology, but for a center-to-center distance of 2 cm. As shown, the coupling factor for the 2-coil inductive link is not sufficient since it stays flat on the entire frequency range of 5 MHz to 30 MHz. For both topologies, the thickness of the biological tissues is considered to be 1 cm (both in measurements and simulation). Indeed, fresh meat (beef) with fat and bone has been used to model the tissues between the repeater coil and the implanted coil. A layer of meet of 1 cm was placed between both coils in the 3-coil structure and clung to the receiver coil in the 2-coil structure. Of course, in a typical application, having the repeater coil outside the body allows tuning the link at the desired resonant frequency to power up the implanted device. Thus, the resonant frequency was tuned by adjusting the repeater coil after having placed the tissues between coils. Such tuning of the repeater can be conducted by varying the coupling factor k_{23}, the size of the coil, or the Q factor of L_2.

Fig. 10 shows the measured and simulated coil coupling factors (k_{12} for the 2-coil structure and k_{13} for the 3-coil structure) for both links as a function of the separation distance (d_{12}). The improvement achieved by the 3-coil link over the 2-coil link is obvious as a larger coupling is obtained for a longer separation distance between the transmitter coil and the receiver coil (between L_1 and L_2 for the 2-coil structure, and between L_1 and L_3 for the 3-coil structure). It should be noted that the real distance between transmitter and receiver coils in the 3-coil structure is one centimeter longer ($d_{13}=d_{12}+1$ cm) than reported in Fig. 10 to account for the separation distance between the repeater coil and the receiver coil.

IV. Conclusion

A transcutaneous power transfer link based on a 3-coil inductive structure has been presented. Such link shows significant improvement over a conventional 2-coil inductive link for transferring power to an implanted device with a high separation distance between the transmitter coil and the receiver coil. Moreover, putting the repeater coil outside the body in such an application allows benefiting from the 3-coil configuration without increasing the size of the implant. Moreover, the resonant frequency or the coil coupling can be adjusted only by changing the size and the quality factor of the repeater coil, which allows optimizing the link after fabrication of the transmitter and receiver coils, as well as after its implantation. The proposed inductive link has been simulated using ADS and HFSS, and verified experimentally.

References

[1] A. Kurs, A. Karalis, R. Moffatt, J. D. Joannopoulos, P. Fisher, and M. Soljacic, "Wireless power transfer via strongly coupled magnetic resonances," *Sci. Expr.* , vol. 317, pp. 83–86, Jul. 2007.

[2] B. L. Cannon, J. F. Hoburg, D. D. Stancil, and S. C. Goldstein, "Magnetic resonant coupling as a potential means for wireless power transfer to multiple small receivers," *IEEE Trans. Power Electron.* , vol. 24, no. 7, pp. 1819–1825, Jul. 2009.

[3] A. K. RamRakhyani, S. Mirabbasi, and M. Chiao, "Design and optimization of resonance-based efficient wireless power delivery systems for biomedical implants," *IEEE Trans. Biomed. Circuits Syst.,* vol. 5, no. 1, pp. 48–63, Feb. 2011.

[4] A. P. Sample, D. A. Meyer, and J. R. Smith, "Analysis, experimental results, and range adaptation of magnetically coupled resonators for wireless power transfer," *IEEE Trans. Ind. Electron.* , vol. 58, no. 2, pp. 544–554, Feb. 2011.

[5] M. W. Baker and R. Sarpeshkar, "Feedback analysis and design of RF power links for low-power bionic systems," *IEEE Trans. Biomed. Circuits Syst.*, vol. 1, no. 1, pp. 28–38, Mar. 2007.

[6] M. Kiani, U. Jow, and M. Ghovanloo, "Design and optimization of a 3-coil inductive link for efficient wireless power transmission," *IEEE Trans. Biomed. Circuits Syst.* , vol. 5, no. 6, pp. 579–591, Dec. 2011.

[7] IEEE Standard for Safety Levels With Respect to Human Exposure to Radio Frequency Electromagnetic Fields, 3 kHz to 300 GHz, IEEE Standard C95.1, 1999.

[8] H. Haus and W. Huang, "Coupled-mode theory," *Proc. IEEE,* vol. 79, no. 10, pp. 1505–1518, Oct. 1991.

[9] U. Jow and M. Ghovanloo, "Modeling and optimization of printed spiral coils in air, saline, and muscle tissue environments," *IEEE Trans. Biomed. Circuits Syst.* , vol. 3, no. 5, pp. 339–347, Oct. 2009.

[10] K. Finkenzeller, RFID-Handbook, 2nd ed. *Hoboken, NJ: Wiley*, 2003.

[11] H. Bahrami, B. Gosselin, and L. A. Rusch, "Design of a Miniaturized UWB Antenna Optimized for Implantable Neural Recording Systems," in *The 10th IEEE NEWCAS Conference (NEWCAS'12)*, Montreal, Canada, June 17, 2012 (Submitted paper).

[12] B. Gosselin, "Recent Advances in Neural Recording Microsystems," Sensors, vol. 11, pp. 4572-4597, 2011.

[13] A. Drossos, V. Santomaa, and N. Kuster, "The Dependence of Electromagnetic Energy Absorption Upon Human Head Tissue Composition in the Frequency Range of 300–3000 MHz," *IEEE Trans. Microw. Theory Tech.*, Vol. 48, No. 11, Nov. 2000.

[14] S. Gabriel, R. W. Lau, and C. Gabriel, "The Dielectric Properties of Biological Tissues: III. Parametric Models for the Dielectric Spectrum of Tissues," *Physics in Medicine and Biology*, Vol. 41, No. 11, pp. 2271–2293, Nov. 1996.